Baryon stopping and hyperon enhancement in the improved dual parton model

A. Capella* and C. A. Salgado†
Laboratoire de Physique Théorique,‡ Université de Paris XI, Bâtiment 210, F-91405 Orsay Cedex, France
(Received 19 March 1999; published 11 October 1999)

We present an improved version of the dual parton model which contains a new realization of the diquark breaking mechanism of baryon stopping. We reproduce in this way the net baryon yield in nuclear collisions. The model, which also considers strings originating from diquark-antidiquark pairs in the nucleon sea, reproduces the observed yields of p and Λ and their antiparticles and underestimates cascades by less than 50%. However, Ω's are underestimated by a factor of 5. Agreement with data is restored by final state interaction, with an averaged cross section as small as $\sigma = 0.14$ mb. Hyperon yields increase significantly faster than antihyperons, in agreement with experiment. [S0556-2813(99)05709-X]

PACS number(s): 25.75.Dw, 24.10.Lx, 24.85.+p

I. INTRODUCTION

A striking feature of heavy ion collisions is the huge stopping of the participating nucleons. At CERN energies, the deep minimum in the net baryon rapidity distribution ($\Delta B = B - \overline{B}$) at $y^* \sim 0$, observed in pp collisions, has been practically filled up in a central collision of heavy ions [1,2]. For central Pb-Pb collisions, the value of this density is five times larger than the corresponding value in pp, scaled by the average number of participants. Note that the total number of $B - \overline{B}$ (i.e., integrated over rapidity), exactly satisfies scaling in the number of participants, due to baryon number conservation. This shows the dramatic change in the shape of the $B - \overline{B}$ (and $p - \overline{p}$) rapidity distributions between pp and central Pb-Pb collisions. Such a change is usually referred to as baryon stopping.

All independent string models of hadronic and nuclear collisions in their original form completely fail to reproduce this important feature of heavy ion collisions. In the dual parton model (DPM) [3] and in the quark gluon string model (QGSM) [4], the dominant contribution to particle production in pp collisions at $\sqrt{s} \sim 20$ GeV, consists of two qq-q strings, which produce, after fragmentation, two baryons in the fragmentation regions of the colliding protons. Starting with the Lund model, which initially had a single string, the above mechanism of particle production has been adopted in most current string models. In these models, there is some amount of stopping due to energy conservation. This produces an increase of the net baryon yield at midrapidities between NN and central Pb-Pb collisions, which is typically of a factor of 2 [3]—more than two times smaller than the observed one. Hence, the dramatic failure of all these models to reproduce the observed stopping.

Actually, a possibility to slow down the net baryon in pp collisions was introduced a long time ago by Rossi and Veneziano [5]. In their approach, the baryon is viewed as three valence quarks bound together by three strings each one with a quark at one end and with the other end joining in a point called string junction. This string junction carries momentum as well as the baryon quantum number. Rossi and Veneziano pointed out that the string junction could migrate to midrapidities with a distribution in $d\sigma/dx \sim 1/\sqrt{x}$ (or $d\sigma/dy \sim \exp(-1/2|(y - y_{\max}|)$. This corresponds to an annihilation cross section which decreases with energy like $s^{-1/2}$. In Refs. [6] and [7] a distribution of the string junction in x^{-1} (i.e., flat in rapidity) was proposed, corresponding to an annihilation cross section which reaches a constant asymptotic value (of 1 to 2 mb). Here we adopt the first approach. However, we do not rule out the second possibility, which would have important consequences at the energies of the future heavy ion colliders [8].

The above stopping mechanism has been recently introduced in heavy ion collisions [8,9] and implemented in the Hijing [10] and Venus [11] Monte Carlo simulations. However, the introduction of the Rossi-Veneziano mechanism does not explain by itself why the stopping is larger in central heavy ion collisions than in pp. In Ref. [8], a mechanism to enhance stopping in heavy ion collisions was proposed. It was based on the separation of the pp cross section $\sigma_{pp} = \sigma_{pp}^{DP} + \sigma_{pp}^{DB}$ into a diquark breaking (DB) and a diquark preserving (DP) piece, and on the assumption that the diquark can be broken in any inelastic collision. These result in a DB cross section in pA and AA collisions which increases faster with A than the DP one. The drawback of this approach is that it requires some fine tuning. The value of σ_{pp}^{DB} has to be small enough in order not to contradict the pp and pA data (where stopping is comparatively small) and large enough to produce the large stopping observed in central heavy ion collisions.

In a recent publication [12], a new formulation of the DB mechanism has been introduced in which this drawback is avoided (i.e., one can have σ_{pp}^{DB} negligibly small at CERN energies, and still have an important effect in central Pb-Pb collisions). In the present paper we use the formulation of [12] to compute the rapidity distributions of $B - \overline{B}$ in hadronic and nuclear collisions. We obtain a reasonable agreement with experiment.[1]

*Electronic address: capella@qcd.th.u-psud.fr
†Electronic address: salgado@qcd.th.u-psud.fr
‡Unité Mixte de Recherche (CNRS) UMR 8627.

[1]Note, however, that similar results are obtained using the approach of Ref. [8] with the DB mechanism of Fig. 2.

Another striking feature of the CERN heavy ion program is the strong increase of the yields of hyperons and antihyperons per participant between *pp* or *pA* and central *AB* collisions. This increase obeys the hierarchy $\Omega > \Xi > \Lambda$ (i.e., the larger the number of strange quarks in *Y*, the larger the increase) [13,14]. In two recent publications [12,15], it has been shown that a baryon stopping mechanism of the type described above produces a substantial increase of the hyperon yields according to this hierarchy. The physical reason for this increase is quite obvious [16]. Since in the diquark breaking component the net baryon is formed out of three sea quarks around the string junction, the probability of producing hyperons is strongly enhanced, especially for Ω's since its probability of production in the conventional diquark fragmentation mechanism is zero. In the present paper we extend the results of [12] in two directions. First, we study the rapidity distributions of protons and hyperons in *pA* and *AA* collisions (in Refs. [12] and [15] the analysis was restricted to the rapidity window $|y^*| < 0.5$). Second, we show how the four free parameters of Ref. [12] can actually be reduced to two. This makes the model more predictive, especially for the antihyperon over hyperon ratios.

While the yield of Λ's and, to a large extent, of cascades can be described by the model, that of omegas is underestimated by almost an order of magnitude. The same conclusion has been reached in [12,15]. We show that final state interaction, with an averaged cross section as small as $\sigma = 0.14$ mb [12], allows one to describe all hyperon and antihyperon yields.

A similar value of σ was found in Ref. [17] in the hadron gas model. It was argued there that, due to this small value of σ, interactions in a hadron gas could not drive the system to chemical equilibrium (the process would be too slow). We find, indeed, that the effect of final state interaction in *p* and Λ production is very small. Its effect on Ξ production is moderate. Only for such a rare process as Ω production is its effect very important, making the $\Omega + \bar{\Omega}$ yield five times larger than the value obtained without final state interaction.

Due to the diquark breaking component, we obtain an increase of hyperons substantially larger than the one of antihyperons, i.e., the ratio between Pb-Pb and *p*Pb yields is substantially larger for *Y* than for $\bar{Y}$. This effect is enhanced by final state interaction. It has been observed experimentally [14].

The paper is organized as follows. In Sec. II we describe the baryon stopping mechanism and compute the net baryon $(B - \bar{B})$ rapidity distributions in *pp*, *p*Pb, *SS* and Pb-Pb collisions. In Sec. III we compute the rapidity distributions of $p - \bar{p}$ and $Y - \bar{Y}$. In Sec. IV we describe $B\bar{B}$ pair production from strings containing sea diquarks or antidiquarks at one of their ends and show how the *A* dependence of $\bar{B}$ production is increased. In Sec. V we study the effect of the final state interaction, separately on the *Y* and $\bar{Y}$ yields. Section VI contains a discussion of our results. Conclusions are given in Sec. VII.

II. BARYON STOPPING

A fragmentation string mechanism in which the $x \to 0$ and $x \to 1$ behavior of the fragmentation functions is controlled by Regge intercepts has been introduced in Ref. [18]. In the case of net baryon production, it consists of a sum of two terms as depicted in Fig. 1. In the original Lund fragmentation scheme [19] only the first term is considered. The second one was introduced later—the so-called popcorn mechanism. Even with the inclusion of the second component [Fig. 1(b)] this mechanism leads to the production of too fast baryons and fails completely to reproduce the observed stopping in heavy ion collisions. This fragmentation scheme [including the component in Fig. 1(b)] will be referred to as the conventional or diquark preserving (*DP*) mechanism. Following Ref. [12] we introduce the baryon stopping mechanism showed in Fig. 2. It will be referred to as the diquark breaking (*DB*) component. In this component, the rapidity distribution of the produced net baryon $\Delta B = B - \bar{B}$ in a *N*-*N* collision is

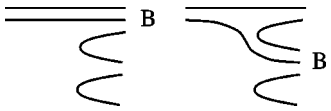

FIG. 1. Conventional diquark preserving (*DP*) fragmentation mechanism for net baryon production.

$$\frac{dN_{DB}^{\Delta B}}{dy}(y) = C_{n_1,n_2}[Z_+^{1/2}(1-Z_+)^{n_1-3/2} + Z_-^{1/2}(1-Z_-)^{n_2-3/2}], \tag{1}$$

where $Z_\pm = \exp(\pm y - y_{\max})$, n_1 and n_2 are the average number of collisions suffered by the two colliding nucleons, and C_{n_1,n_2} is determined from the normalization to two. The factor $Z^{1/2}$ has already been discussed in the Introduction. The factor $(1-Z)$ gives the behavior near $y = y_{\max}$. There is some uncertainty concerning its power [8]. The value in Eq. (1) is obtained as follows. From Fig. 2 we see that in order to produce the baryon at $y \sim y_{\max}$ it is necessary to slow down three quarks. Assuming they behave as $1/\sqrt{x}$ at the energies under consideration [4], we obtain a power 1/2 for the case of Fig. 2, which corresponds to $n = 2$. In the general case of *n* inelastic collisions we obtain the power $n - 3/2$ in Eq. (1).

The corresponding distribution in *AA* collisions is [12]

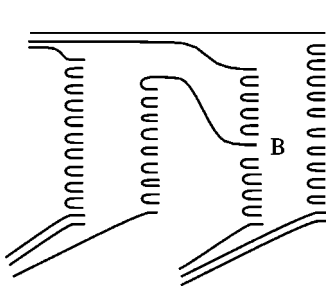

FIG. 2. Example of diquark breaking (*DB*) diagram for net baryon production in *pA* with two inelastic collisions.

$$\frac{dN^{AA\to\Delta B}}{dy}(y)=\frac{\overline{n}_A}{\overline{n}}\left[\overline{n}_A\left(\frac{dN^{\Delta B}_{DP}}{dy}(y)\right)_{\overline{n}/\overline{n}_A}+(\overline{n}-\overline{n}_A)\times\left(\frac{dN^{\Delta B}_{DB}}{dy}(y)\right)_{\overline{n}/\overline{n}_A}\right]. \quad (2)$$

Here $\overline{n}_A$ and $\overline{n}$ are the average number of participants of nucleus A and the average number of collisions, respectively. dN_{DP}/dy is given by the conventional, diquark preserving, hadronization mechanism for which we use the results of Ref. [20], and dN_{DB}/dy is given by Eq. (1). The integral over y of both rapidity distributions is equal to two (baryon number conservation).

Let us discuss the physical meaning of Eq. (2) in pp interactions ($\overline{n}_A=1$). We see that in the case of a single inelastic collision ($\overline{n}=1$), we recover the conventional DP mechanism. The underlying assumption is that, in this case, the string junction follows the valence diquark and baryon production takes place in the conventional way. (We do not exclude a small admixture of the DB component in this case, but experimental data do not require its presence. This smallness can be due to the fact that in this case, the corresponding graph has three strings [9]. This configuration, the same as in $p\overline{p}$ annihilation, is not the dominant one, which in DPM consists of two strings.) Consider next the case of two inelastic collisions ($\overline{n}=2$). Here the underlying assumption is that there is an equal probability (1/2) for the net baryon to be produced in any of the two collisions. However, in only one of them can the string junction follow the valence diquark and fragment in the conventional (DP) way. In the other one, the string junction is free and baryon production takes place according to the DB mechanism. (In this case the diagram, Fig. 2, is the one corresponding to the dominant configuration: four strings.) The DB component is responsible for (most of) the observed baryon stopping. The generalization to $\overline{n}$ inelastic collisions and to AA interactions [Eq. (2)] is then straightforward. The probability of DP is $\overline{n}_A/\overline{n}$ and the one of DB is $1-\overline{n}_A/\overline{n}=(\overline{n}-\overline{n}_A)/\overline{n}$. The extra factor of $\overline{n}_A$ in Eq. (2) is necessary to ensure baryon number conservation.

It is quite remarkable that such a simple mechanism, with no free parameter [modulo the uncertainty in the power of $1-Z$ in Eq. (1), discussed above] gives a good description of the present data on the net baryon rapidity distribution.

Note that in the case of pp interactions at $\sqrt{s}\sim 20$ GeV, the two string component ($\overline{n}=1$) dominates, and, as discussed above, we recover the usual DP results. With increasing energies, the components with $\overline{n}\neq 1$ become increasingly important and baryon stopping will increase. Equation (1) (with $\overline{n}_A=1$) not only gives definite predictions concerning this increase but, moreover, leads to specific qualitative features. In particular stopping will strongly depend on the charged particle multiplicity. A low multiplicity event sample selects low values of $\overline{n}$ where stopping will be comparatively small, while, at large multiplicities, stopping will be larger. Such a feature has been observed recently at HERA [21], and discussed in Ref. [22] in a different theoretical framework.

We turn next to the generalization of Eq. (2) to asymmetric interactions such as pA. In this case one has

$$\frac{dN^{pA\to\Delta B}}{dy}(y)=\frac{dN^{qq^A-q^p_v}_{DP}}{dy}(y)+(\overline{n}-1)\frac{dN^{qq^A-q^p_s}_{DP}}{dy}(y)+\frac{1}{\overline{n}}\left[\frac{dN^{q^A_v-qq^p}_{DP}}{dy}(y)+(\overline{n}-1)\times\frac{dN^{q^A_v-qq_p}_{DB}}{dy}(y)\right]. \quad (3)$$

Here $dN^{qq^A-q^p_v(q^p_s)}/dy$ denotes the rapidity distribution of a string stretched between a diquark of one of the $\overline{n}$ wounded nucleons of A and a valence (or sea) quark of the proton. (It is computed in DPM as a convolution of momentum distribution functions and fragmentation functions.) Since each of the wounded nucleons suffers a single inelastic collision, only the DP component is involved, with each diquark fragmenting in the nucleus fragmentation region ($y^*<0$). The terms in the bracket correspond to the fragmentation of the incoming proton. Since it suffers $\overline{n}$ inelastic collisions, we have the DP hadronization mechanism (with probability $1/\overline{n}$) and the DB one [with probability $(\overline{n}-1)/\overline{n}$]. The latter is now given by the first term of Eq. (1). All rapidity distributions, integrated over y, are equal to one in this case.

The $B-\overline{B}$ rapidity distributions obtained from Eq. (2) in central SS and Pb-Pb collisions are shown in Fig. 3. Note that at midrapidities, these distributions are dominated by the DB component. Not only the latter is proportional to $\overline{n}-\overline{n}_A$ [Eq. (2)], but, moreover, dN_{DB}/dy is larger than dN_{DP}/dy at midrapidities (see Table I). Nevertheless, the existence of the two huge maxima of the DP component in the fragmentation regions, still shows up in the AA distribution. For a given system, the detailed shape of the $B-\overline{B}$ rapidity distribution depends on the power of $(1-Z)$ in Eq. (1). As discussed above there is some theoretical uncertainty in the value of this power. However, the variation of the shape of this rapidity distribution from one system to another is a characteristic feature of the model. As seen in Fig. 3, the minimum at midrapidities is gradually filled up from pp to central Pb-Pb collisions and, therefore, it is more pronounced in SS than in Pb-Pb.

III. NET HYPERON ENHANCEMENT

In the previous section we have shown that baryon stopping can be described using a new formulation of the diquark breaking (DB) mechanism. In this case, depicted in Fig. 2, the string junction is surrounded by three sea quarks to produce the net baryon. Therefore, not only the net proton yield $\Delta p=p-\overline{p}$ will be strongly enhanced from pp to central AA collisions, but also the net hyperon yield $\Delta Y=Y-\overline{Y}$. This is especially so for Ω's, which cannot be produced at all with

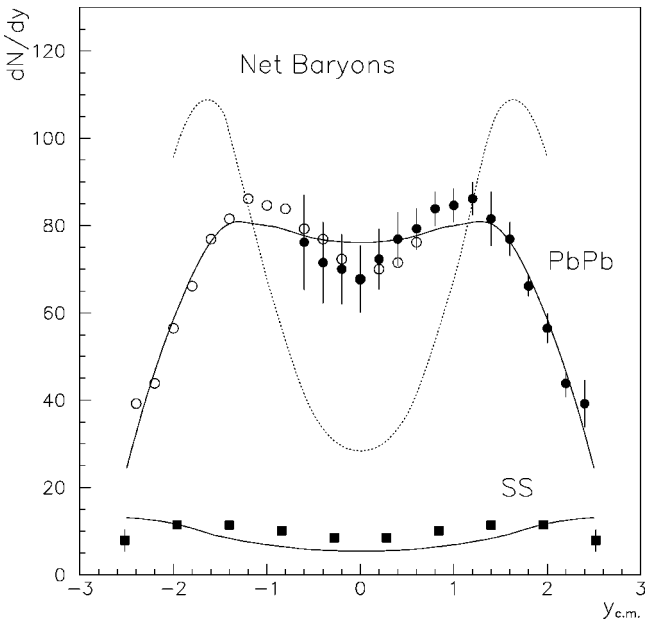

FIG. 3. Rapidity distribution of the net baryon number $(B-\overline{B})$ in central *SS* (200*A* GeV/*c*) and PbPb (158*A* GeV/*c*) collisions. The full lines are obtained from Eq. (2). The data are from Refs. [1, 2] [for central *SS* collisions the data are obtained as $B-\overline{B}=2(p-\overline{p})+1.6(\Lambda-\overline{\Lambda})$]. Open circles are data reflected about $y^*=0$ (errors not shown). The dotted line is the result obtained without the *DB* component in the case of central PbPb collisions. Due to baryon number conservation, these results are not affected by final state interactions.

the *DP* mechanism of Figs. 1(a) and 1(b).[2] More precisely the ratio between yields in central *AA* and *pA* (or *pp*) collisions will obey the hierarchy $\Delta\Omega>\Delta\Xi>\Delta\Lambda>\Delta p$. This is in agreement with the results of the WA97 [14] and NA49 [1,13] Collaborations.

The relative yields of the different baryon species will be determined by the strangeness suppression factor S/L where S is the probability associated to the strange quark and L the one associated to the light quarks (u or d). We consider two possibilities: $S=0.10$ and $L=(1-S)/2=0.45$ ($S/L=0.22$) and $S=0.13$ and $L=0.435$ ($S/L=0.3$). With baryons produced out of three sea quarks (Fig. 2) it is easy to see that the relative yields are

$$I_3=4L^3{:}4L^3{:}12L^2S{:}3LS^2{:}3LS^2{:}S^3 \qquad (4)$$

for p, n, $\Lambda+\Sigma$, Ξ^0, Ξ^-, and Ω, respectively. Moreover, we take, $\Sigma^++\Sigma^-=0.6\Lambda$. This reduction in the number of charged Σ's is due to resonance decay ($\Sigma(1385)P_{13}$ decays into $\Lambda\pi$ with an $88\pm2\%$ fraction).

[2]A new component consisting in a diquark which contains sea quarks has been introduced in [23]. However, this diquark is assumed to have the same momentum distribution as a diquark made out of two valence quarks and, hence, produces baryons mainly in the fragmentation regions.

TABLE I. Values of the rapidity densities at $y^*=0$ in Eqs. (2) and (7) for central PbPb collisions ($\overline{n}_A=178$, $\overline{n}=858$) with $\alpha=0.23$ and $S/L=0.3$ (first four lines), and with $\alpha=0.5$ and $S/L=0.22$ (last two lines). The *DP* and string contributions are the same in both cases. The value of the *DP* component for Ξ^- is not exactly 0, due to the fragmentation mechanism of Fig. 1(b). However, its value is very small as compared to the other components and has been neglected.

	p	Λ	Ξ^-	Ω
$dN^{\overline{B}}_{\rm sea}/dy$	4.80×10^{-3}	2.15×10^{-3}	3.21×10^{-4}	3.20×10^{-5}
$dN^{\Delta B}_{DB}/dy$	9.12×10^{-2}	3.00×10^{-2}	2.86×10^{-3}	1.23×10^{-4}
$dN^{\Delta B}_{\overline{D}P}/dy$	6.90×10^{-2}	1.40×10^{-2}	0	0
$dN^{B}_{\overline{\rm string}}/dy$	8.50×10^{-3}	2.26×10^{-3}	1.65×10^{-4}	5.07×10^{-6}
$dN^{B}_{\rm sea}/dy$	6.54×10^{-3}	2.43×10^{-3}	2.98×10^{-4}	2.4×10^{-5}
$dN^{\Delta B}_{DB}/dy$	9.56×10^{-2}	2.62×10^{-2}	2.29×10^{-3}	1.23×10^{-4}

It is interesting that, in spite of the huge hyperon enhancement observed experimentally, the factors (4) lead (both with $S=0.10$ and $S=0.13$) to an overestimation of hyperon production in pPb collisions especially for Ξ's and Ω's. In central Pb-Pb collisions, net hyperon production is also overestimated, except for Ω's. In Ref. [12] the following explanation of this hyperon excess was proposed: at present energies, it may happen that the net baryon is not formed out of three sea quarks as in Fig. 2, but, due to phase space

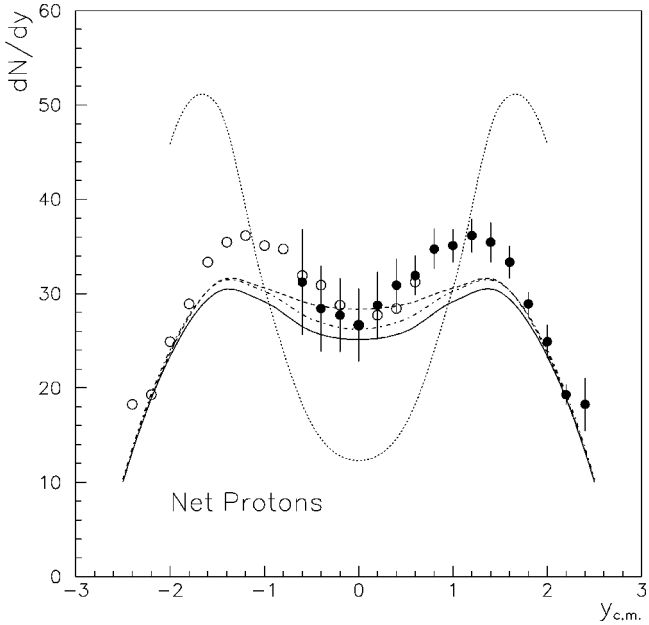

FIG. 4. Rapidity distributions for net proton production $(p-\overline{p})$ in central PbPb collisions at 158*A* GeV/*c* compared to the results of Ref. [1]. Open circles are data reflected about $y^*=0$ (errors not shown). The dashed line is our result without final state interactions with a strangeness suppression factor $S/L=0.3$, and the full line is the corresponding result with final state interactions. The dotted-dashed line corresponds to a suppression factor $S/L=0.22$ and with final state interactions. The dotted line is our result without the *DB* component and without final state interactions.

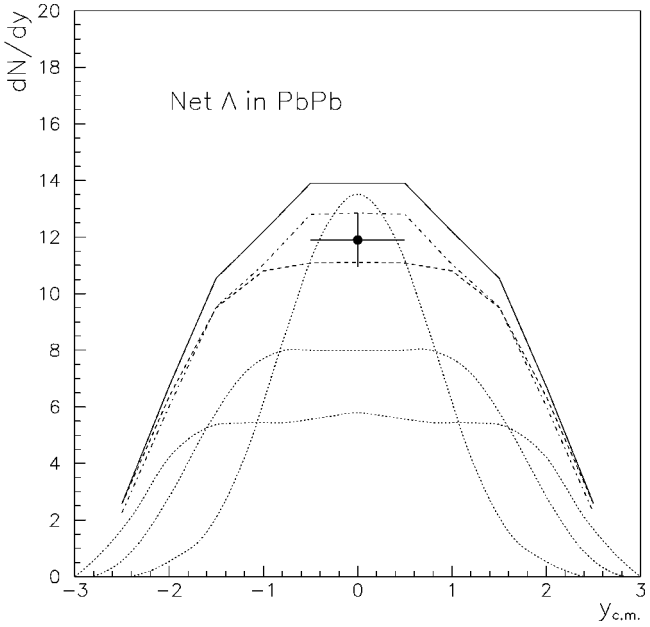

FIG. 5. Same as Fig. 4 for $\Lambda-\overline{\Lambda}$. Now the three dotted lines are estimates by the NA49 Collaboration [1]. The experimental point at $y^*=0$ is from the WA97 Collaboration [14].

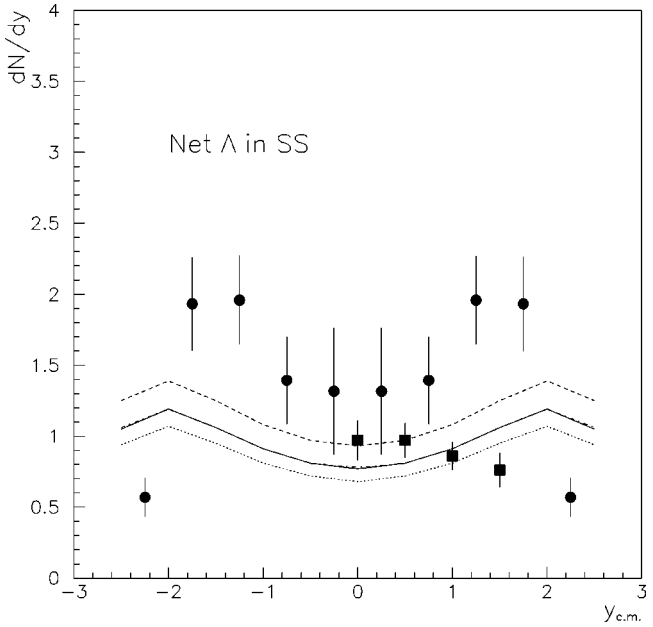

FIG. 6. Same as Fig. 5 for central *SS* collisions. The data are from NA35 [2] (circles). Also shown, the value of the total Λ yield measured by NA36 [32] (squares). The theoretical curves are computed with: $\alpha=0.23$, $S/L=0.3$ (full line); $\alpha=1$, $S/L=0.3$ (dashed line); $\alpha=0.23$, $S/L=0.22$ (dotted line) and $\alpha=1$, $S/L=0.22$ (dashed-dotted line).

limitation, a valence quark, at one of the ends of the string where the baryon is produced, is picked up together with two sea quarks. Obviously, in this case the strangeness production rate is substantially reduced (in particular, Ω production is not possible in this case). The relative yields I_3 in (4) are then changed into

$$I_2=2L^2{:}2L^2{:}4LS{:}S^2/2{:}S^2/2{:}0. \tag{5}$$

Note that the rapidity distribution of the net baryon is taken to be the same for the two mechanisms described above. The idea is that this distribution is given in both cases by the probability to slow down the string junction, Eq. (1), and that a valence quark is picked up only when it happens to be close by in rapidity.

In the following, we introduce a free parameter α ($0<\alpha<1$) which determines the admixture of I_3 and I_2 given by Eqs. (4) and (5). More precisely, we will take the relative yields given by

$$I=\alpha I_3+(1-\alpha)I_2. \tag{6}$$

The best description of the data is obtained with $\alpha=0.23$ for $S=0.13$ and $\alpha=0.5$ for $S=0.1$. The results are similar in the two cases, the sensitivity to the value of the strangeness suppression factor S/L turns out to be quite small. The results for the rapidity distribution of the net yields of p and Λ in central Pb-Pb collisions are given in Figs. 4 and 5. Note that our rapidity distribution for $\Lambda-\overline{\Lambda}$ (Fig. 5) is broader than the estimates of the NA49 Collaboration [1]. This, in turn, produces some discrepancies in the $p-\overline{p}$ yield (Fig. 4). Final data on Λ and $\overline{\Lambda}$ are needed in order to clarify the situation, we shall come back to this point in Sec. VI. The net Λ rapidity distribution in central *SS* collisions is shown in Fig. 6. The corresponding results for minimum bias *pA* collisions are given in Figs. 7 and 8. It is seen that the normalization of the experimental data is larger than the theoretical one, especially for $p-\overline{p}$. Note, however, that by integrating over y the experimental distributions one realizes that their normalization is larger than the number of wounded nucleus in *pAu* (given by the Glauber model) by more than a factor of 2. As

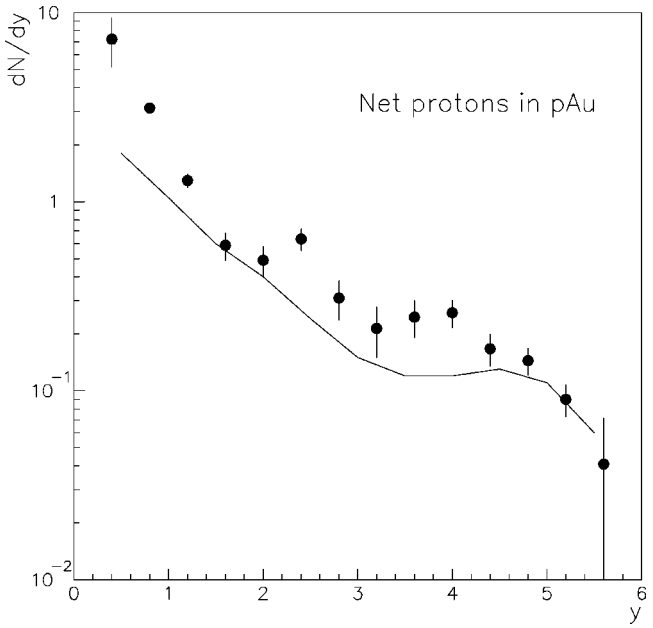

FIG. 7. Same as Fig. 4 for minimum bias *pAu* interactions. The experimental data are from Ref. [2].

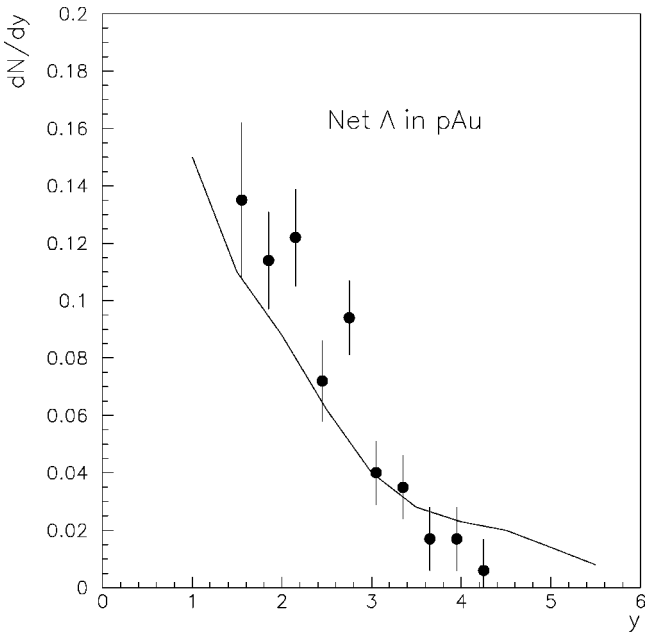

FIG. 8. Same as Fig. 5 for minimum bias *pAu* interactions. The experimental data are from Ref. [2].

pointed out in [2] this excess may be due to recoil nucleons which are not completely disentangled from the wounded ones. This point needs clarification.

Note that, in our model, the relative yields I_3 [Eq. (4)] should apply at higher energies when the phase space limitations are less important. With $S/L=0.3$, they would give a ratio $\Xi^+ + \Xi^0/\Lambda+\Sigma \sim 0.3$ which is in agreement with Fermilab [24] and SPS collider data [25].

IV. ANTIBARYON PRODUCTION

In string models, $B\overline{B}$ pair production takes place via diquark-antidiquark pair production in the string fragmentation. It turns out that at present CERN energies only strings of type qq-q have large enough invariant mass to produce $B\overline{B}$ pairs. This gives rise to a scaling of $\overline{B}$ yields in the number of participants. (The number of qq-q strings is proportional to the number of wounded nucleons.) Experimentally, the observed increase is much faster—closer to a scaling in the number of collisions. In order to solve this problem it was proposed some time ago [20,26,27] to consider the production of $B\overline{B}$ pairs from diquark-antidiquark pairs in the sea of the participating nucleons.[3] The rapidity distribution of antibaryons in *AA* collisions is then given by

$$\frac{dN^{AA\to\overline{B}}}{dy}(y)=\overline{n}_A\left(\frac{dN^{\overline{B}}_{\rm string}}{dy}(y)\right)_{\overline{n}/\overline{n}_A}+(\overline{n}-\overline{n}_A)\times\left(\frac{dN^{\overline{B}}_{\rm sea}}{dy}(y)\right)_{\overline{n}/\overline{n}_A}. \tag{7}$$

The first term represents the conventional pair production in the string breaking process. As discussed above, it is proportional to the number of participants. The second term corresponds to pair production from a string having a sea diquark or antidiquark at one of their ends. In DPM, the total number of strings is proportional to $\overline{n}$. Since the number of strings with a valence diquark at one of their ends is proportional to $\overline{n}_A$, the number of strings with a sea diquark at one of their ends is proportional to $\overline{n}-\overline{n}_A$. Of course, pulling a diquark-antidiquark pair out the nucleon sea is dynamically suppressed, in the same way as its production in the string breaking process is suppressed as compared to q-$\overline{q}$ production. Thus, we expect that in each individual string, the production of $B\overline{B}$ pairs in the two components (sea and string) in Eq. (7) are comparable. In practice, the normalization of the second component is treated as a free parameter. However, it turns out that the sea component is always smaller than the string one, not only at $y^*=0$ (see Table I) but also after integration over rapidity. Note that the string with sea diquarks have a smaller invariant mass.

For the string term we use the results of Ref. [20]. The absolute normalization of this term was determined from a fit of the *pp* data. For the *y* dependence of the sea term, we also use the results of Ref. [20]. As discussed above, its absolute normalization is a free parameter. This parameter is the same for all species of baryons. More precisely, since the baryons and antibaryons in the sea component are made out of three sea quarks or antiquarks, the relative yields of the different baryon species is again given by Eq. (4).[4] (We neglect here the small differences in the rapidity shapes induced by the different baryon masses.) We are left in this way with a single free parameter for this new sea component. Therefore, we have a total number of two free parameters, one in the diquark breaking component and one in the sea component, plus the value of the strangeness suppression factor S/L for which two values (0.22 and 0.3) have been considered. Of course, the conventional components *DP* and string in Eqs. (2) and (7) contain several free parameters. However, as discussed above, these parameters have been fixed in Ref. [20] from a fit of the *pp* data and are not changed here.[5] The values at $y^*=0$ of the various components for the different baryon species are given in Table I.

The results for the rapidity distributions of the $\Lambda+\overline{\Lambda}$, $\Xi^-+\Xi^+$, Ξ^-, and $\Omega+\overline{\Omega}$ yields in central Pb-Pb collisions at 158 GeV are given in Figs. 9–12. The p, $\overline{p}$, Y, and $\overline{Y}$ yields at $|y^*|<0.5$ in minimum bias pPb collisions as well as at four different centralities in Pb-Pb collisions, are given in Fig. 13. The corresponding ratios $R_Y=\overline{Y}/Y$ at $|y^*|<0.5$ are given in Fig. 14. It should be noted that the values of R_Y are not absolute predictions of our model. They can be

[3]A different mechanism based on string junction-antijunction exchange has been proposed recently [15].

[4]Note that in this case $\alpha=1$; i.e., no admixture of the type discussed in connection with the *DB* component is present here.

[5]For this reason, the change in the strange suppression parameter S/L from 0.22 to 0.3 only applies to the new components *DB* and sea in Eqs. (2) and (7) (see Table I).

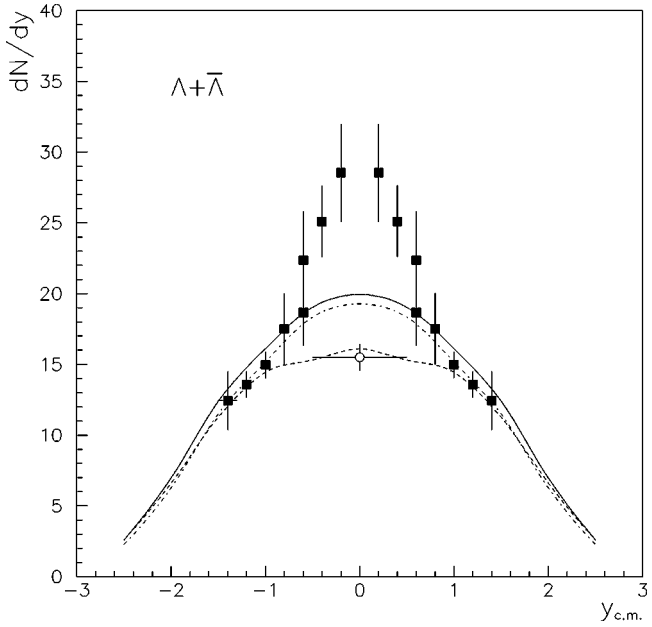

FIG. 9. Same as Fig. 4 for $\Lambda+\overline{\Lambda}$. The point at $y^*=0$ (circle) is from the WA97 Collaboration [14]. The squares are from NA49 [1].

changed by changing the normalization of the sea component in Eq. (7). However, the ratios $R_p:R_\Lambda:R_\Xi:R_\Omega$ are a characteristic feature of the model. They show an increase with the number of strange quarks in the baryon. In Fig. 15 we show the various baryon yields at $y^*=0$ divided to the average number of participants, $2\overline{n_A}$, normalized to the same quantity in pPb. A discussion of these results is given in Sec. VI, after introducing final state interaction.

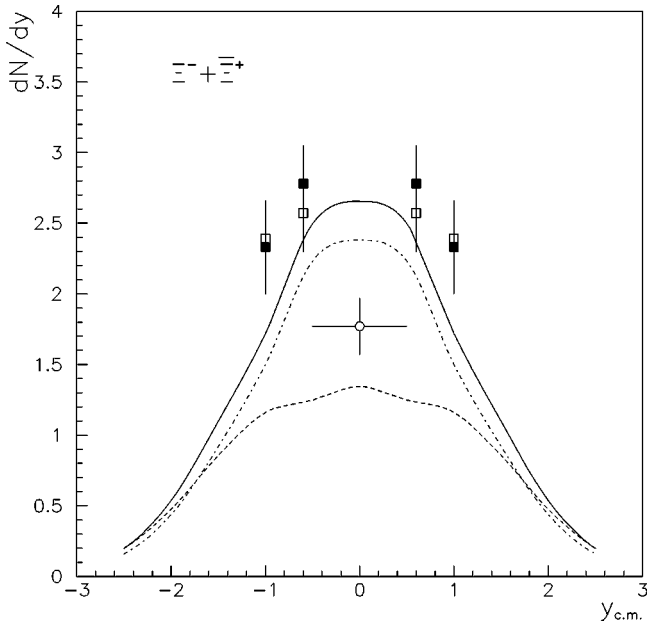

FIG. 10. Same as Fig. 9 for $\Xi^-+\overline{\Xi}^+$. The NA49 data are from Ref. [13].

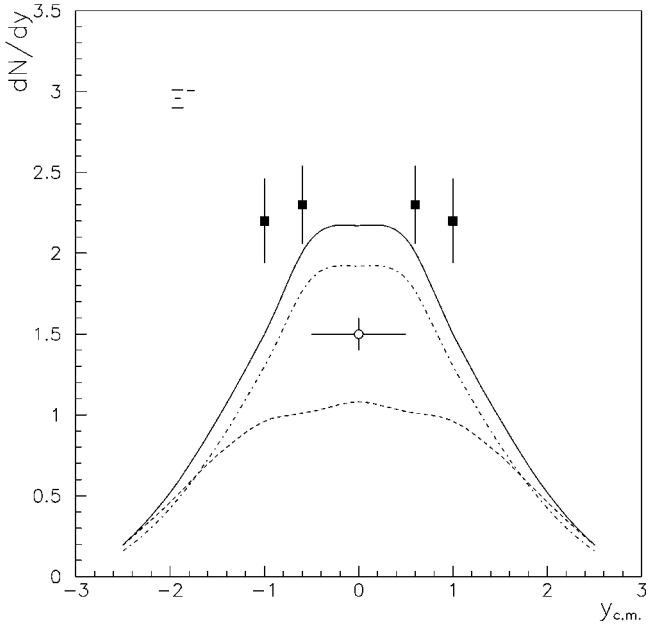

FIG. 11. Same as Fig. 9 for Ξ^-. The NA49 data are from Ref. [13].

V. FINAL STATE INTERACTION

In an attempt to explain the strong enhancement of the $\Omega+\overline{\Omega}$ yield observed by the WA97 Collaboration [14], we are going to use our results for the baryon densities as initial conditions in the gain and loss differential equations which govern final state interactions [17,28]

$$\frac{dN_i}{d^4x}=\sum_{k,l}\ \sigma_{kl}\rho_k(x)\rho_l(x)-\sum_k\ \sigma_{ik}\rho_i(x)\rho_k(x). \qquad (8)$$

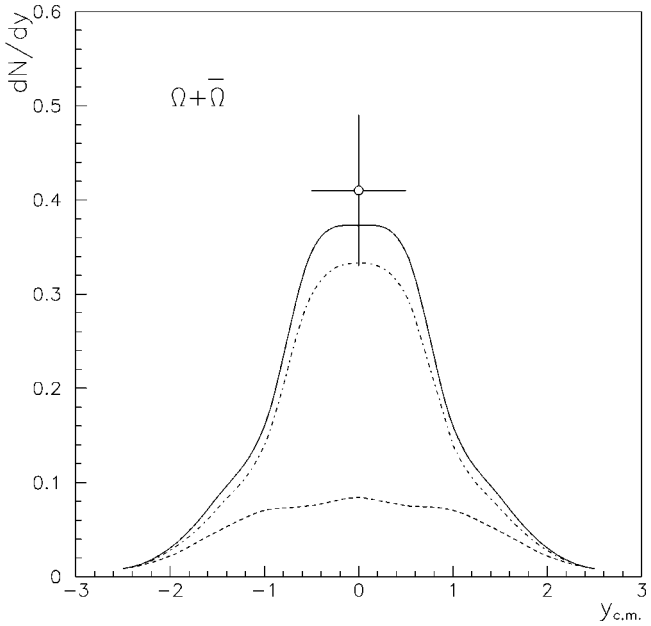

FIG. 12. Same as Fig. 9 for $\Omega+\overline{\Omega}$. The experimental point is from WA97 [14].

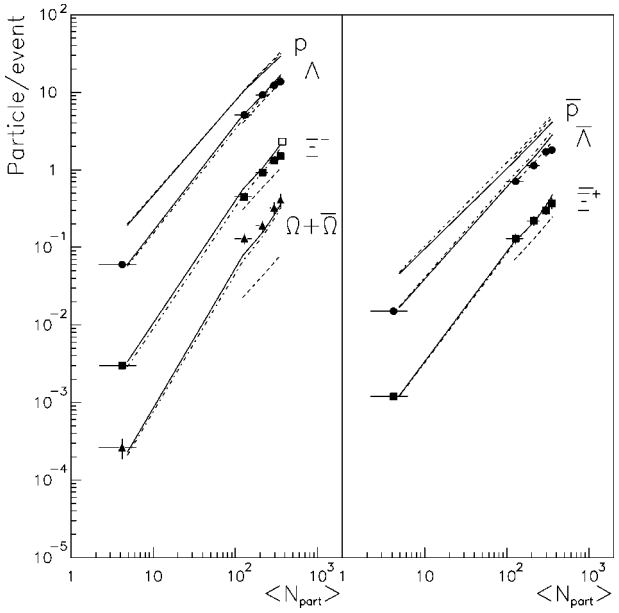

FIG. 13. Yields of p, Λ, Ξ^-, $\Omega+\overline{\Omega}$, $\overline{p}$, $\overline{\Lambda}$, and $\overline{\Xi}^+$ for minimum bias pPb (158 GeV/c) and central PbPb collisions (158A GeV/c) in four centrality bins. Experimental data are from WA97 [14] (black points) and NA49 [13] (open square). Full (dashed) lines are our results with (without) final state interactions for strangeness suppression factor $S/L=0.3$. The dashed-dotted lines are our results with final state interactions for $S/L=0.22$.

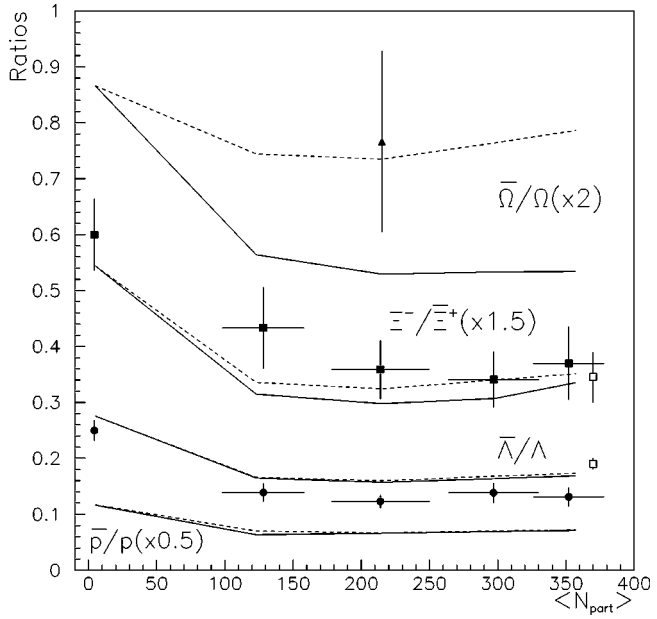

FIG. 14. Ratios $\overline{B}/B$ at $y^*=0$ for minimum bias pPb and PbPb collisions in four different centrality bins at 158A GeV/c. Black circles, squares, and the triangle correspond to experimental data of WA97 [14] for $\overline{\Lambda}/\Lambda$, $\overline{\Xi}^+/\Xi^-$, and $\overline{\Omega}/\Omega$, respectively. Open squares are NA49 data [13]. Full lines are our results with final state interactions and dashed lines without final state interactions, both for $S/L=0.3$.

The first term on the right-hand side of Eq. (8) describes the production of particles of type i resulting from the interaction of particles k and l with space-time densities $\rho(x)$ and cross sections σ_{kl} (averaged over the momentum distribution of the interacting particles). The second term describes the loss of particles of type i due to its interaction with particles of type k. We use cylindrical space-time variables and assume boost invariance [i.e., the densities $\rho(x)$ are taken to be independent of y]. If we furthermore assume that the dilution in time of the densities is mainly due to longitudinal motion, i.e.,

$$\rho_i(\tau,y,\vec{s})=\rho_i(\tau,\vec{s})\,\frac{\tau_0}{\tau}, \tag{9}$$

where $\tau=\sqrt{t^2-z^2}$ is the proper time and $\vec{s}$ the transverse coordinate, Eqs. (8) can be written as [28]

$$\tau\frac{d\rho_i}{d\tau}=\sum_{k,l}\ \sigma_{kl}\rho_k\rho_l-\sum_k\ \sigma_{ik}\rho_i\rho_k\,. \tag{10}$$

Here $\rho_i(y,\vec{s},\vec{b})=dN_i/dyd\vec{s}d\vec{b}$. Thus, at fixed impact parameter $\vec{b}$, we have to know the rapidity densities per unit of transverse area $d\vec{s}$. Our Eqs. (2) and (7) do give these rapidity densities—the dependence on $\vec{s}$ and $\vec{b}$ is contained in the geometrical factors $\overline{n_A}$ and $\overline{n}$, given by the Glauber model. In the following, we use nuclear profiles obtained from Woods-Saxon nuclear densities using the three-parameter Fermi distribution of Ref. [29]. For the pion densities we use the DPM results of Ref. [30], where explicit expressions as a function of $\overline{n_A}$ and $\overline{n}$ are given.

Equations (10) have to be integrated from initial time τ_0 to freeze-out time τ. These equations are invariant under the change $\tau\rightarrow c\,\tau$. Therefore the result depends only on the ratio

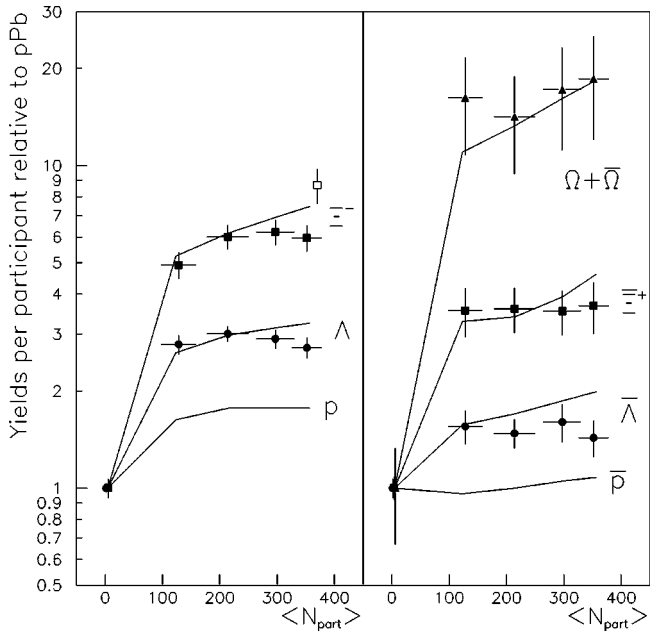

FIG. 15. Same as Fig. 14 for the baryon yields at $y^*=0$ in PbPb divided by the number of participant nucleons relative to the same ratio in minimum bias pPb.

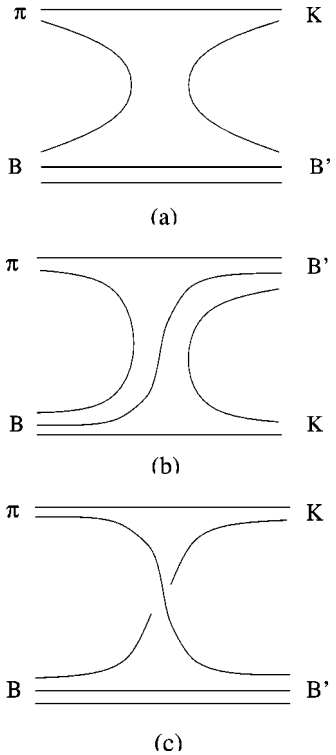

FIG. 16. (a) Quark diagrams for reactions (11) with light quark pair annihilation and $s-\bar{s}$ quark creation. (b) Quark diagram for reactions (11) with three quark exchange in the t channel. (c) Quark diagram for strangeness exchange reactions.

τ/τ_0. Following Refs. [30, 31], we use the (inverse) proportionality between τ and ρ and put $\tau/\tau_0=\rho(y,\vec{s},\vec{b})/\rho_{f_0}$. Here $\rho(y,\vec{s},\vec{b})$ are the initial densities given by our expressions obtained in previous sections and ρ_{f_0} is the freeze-out density. For the latter, we take the charged density per unit rapidity in a pp collision, i.e., $\rho_{f_0}=[3/\pi R_p^2](dN^-/dy)_{y*=0}=1.15\,\mathrm{fm}^{-2}$ [30,31].

We now have to specify the channels that have been taken into account in our calculation. They are

$$\pi N\to K\Lambda,\quad \pi N\to K\Sigma,\quad \pi\Lambda\to K\Xi,\quad \pi\Sigma\to K\Xi,$$

$$\pi\Xi\to K\Omega, \tag{11}$$

and the corresponding reactions for antiparticles. To be more precise, of all possible charge combinations in Eq. (11), some are of the type shown in Fig. 16(a), with annihilation of a light quark pair and production of an $s-\bar{s}$. They have all been taken into account with the same cross section $\sigma=0.14\,\mathrm{mb}$. All other reactions in Eq. (11) are of the type shown in Fig. 16(b). They have three quark lines in the t channel (baryon exchange). Their average cross section is smaller than the one of Fig. 16(a) and has been neglected.[6] We have also neglected all strangeness exchange reactions [Fig. 16(c)] $KN\leftrightarrow\pi\Lambda$, etc. Although the corresponding cross sections are larger at threshold, this is no longer the case for the cross sections averaged over the momentum distributions of the interacting particles. (This is due to their steep decrease with increasing energy, see [17].) Channels (11) are thus dominant due to the relations $\rho_N>\rho_\Lambda>\rho_\Xi>\rho_\Omega$ and $\rho_\pi>\rho_K$ between particle densities. The results, obtained after solving numerically Eqs. (10), with our initial densities and a common value of the averaged cross section $\sigma=0.14\,\mathrm{mb}$ for all channels, are shown in our figures by a full line in the case $S/L=0.3$ and $\alpha=0.23$ and by a dashed-dotted line in the case $S/L=0.22$ and $\alpha=0.5$. (A comparable value of σ has been obtained in Ref. [17] in a hadron gas model.)

The effect of the final state interaction is negligibly small in pA collisions. In central SS collisions its effect on the p and Λ yields is very small (less than 5%). The effect increases with the number of strange quarks in the produced hyperon. In central Pb-Pb collisions, with our value of the cross section, it turns out to be comparatively small for p and Λ yields. However, it increases the Ξ yields by up to 50% and the $\Omega+\bar{\Omega}$ yield by a factor of 5. Agreement with the WA97 data [14] is obtained in this way (Fig. 13).

It is important to note that, due to the small value of σ, the final state interaction has an important effect only on very rare processes such as Ω production. It cannot drive the system into chemical equilibrium, even locally.

VI. DISCUSSION

We discuss here the main features of our results. For $\Lambda+\bar{\Lambda}$ our results for Pb-Pb are slightly higher than the WA97 data and grossly underestimate NA49 ones at midrapidities (Fig. 9). Note, however, that the latter are very preliminary and are currently under reanalysis. For central SS collisions, where the NA35 data are final, we slightly underestimate their net Λ yield and slightly overestimate the total Λ yield form NA36 [32] (Fig. 6). However, the NA35 value for the $\bar{\Lambda}$ yield at midrapidities 0.75 ± 0.15 is about two times larger than our result. Note that this experimental point looks ''anomalous'': compared with the WA97 value for the most central rapidity bin in Pb-Pb collisions, (1.8 ± 0.2), there is an increase by a factor of 2.4, whereas the number of participants increases by a factor of 7. Note also that NA35 finds a ratio $\bar{\Lambda}/\bar{p}=1.9\pm0.7$ at midrapidities, while in our model

[6]The reactions we have kept are $\pi^++n\to K^+\Lambda$, $\pi^-p\to K^0\Lambda$, $\pi^-+n\to K^0\Sigma^-$, $\pi^+p\to K^+\Sigma^+$, $\pi^-\Lambda\to K^0\Xi^-$, $\pi^+\Lambda\to K^+\Xi^0$, $\pi^+\Sigma^-\to K^+\Xi^-$, $\pi^-\Sigma^+\to K^0\Xi^0$, $\pi^-\Xi^0\to K^0\Omega$, and $\pi^+\Xi^-\to K^+\Omega$ for the reactions initiated by π^+ or π^-. For all of them, as well as for the corresponding ones with antiparticles, we take $\sigma=0.14\,\mathrm{mb}$. The reactions initiated by π^0 are either of the type of Figs. 16(a) or 16(b), depending on whether the $u\bar{u}$ or $d\bar{d}$ component of the π^0 is considered. For this reason all these reactions have been included with cross section $\sigma/2$.

this ratio is always smaller than one (see Fig. 13). This important point needs clarification. In particular, final values of this ratio in Pb-Pb collisions are needed.

The NA49 data concerning the cascade yield are published [13]. They are 30–40% higher than the WA97 ones [14] at midrapidities. Our results, after final state interaction, are intermediate between the two sets of data, but somewhat closer to the NA49 results (Figs. 10 and 11). The $\Omega+\overline{\Omega}$ yields are in agreement with the WA97 data, after final state interaction (Fig. 12 and 13).

As discussed in Sec. IV, in our model, the ratios $R_Y = \overline{Y}/Y$ increase with the number of strange quarks in the baryon (Fig. 14). This tendency is also seen in the data. However, the ratio of ratios R_Ξ / R_Λ is somewhat too small in our model as compared to the WA97 data [14], but agrees with the NA49 ones [1,13]. (Remember, however, that the value of R_Λ from NA49 is preliminary.)

Another characteristic feature of our approach is that, at midrapidities, hyperons are more strongly enhanced than antihyperons. As a consequence, the ratio $\overline{Y}/Y$ decreases between pPb and central Pb-Pb collisions (Fig. 14). This is due to the strong effect of the *DB* component in the net baryon yield. Final state interaction works in the same direction. This important feature of our results is seen in the data [14].

Finally, the WA97 Collaboration has found that the increase of the hyperon and antihyperon yields per participant (Fig. 15) increases faster than the number of participants between pPb and the first centrality bin in Pb-Pb. However, between the first and last centrality bin all yields approximately scale with the number of participants. We find an increase which is faster in the first case than in the second one. However, some mild increase is left in Pb-Pb (Fig. 15).

VII. CONCLUSIONS

The large baryon stopping observed in central heavy ion collisions at CERN energy is not reproduced by any of the available independent string models, at least in their original form. We have modified the DPM by introducing a new realization of the diquark breaking mechanism. We reproduce in this way the observed net baryon yield. This mechanism also produces an important enhancement of net hyperons. At this level, the new version of DPM presented here (which has also diquark-antiquark pairs in the nucleon sea) remains strictly an independent string model. It reproduces with two free parameters, the observed yields of p and Λ and their antiparticles in pA and Pb-Pb collisions. Cascades in central Pb-Pb collisions are underestimated by less than 50% while Ω's are too small by a factor of 5. Agreement with experiment is restored by introducing final state interaction with an averaged cross section as small as $\sigma = 0.14$ mb. In this way, we depart from string independence. However, with this small value of the cross section, there is no significant effect on the bulk of particle production. A comparable value of the cross section for final state interaction was obtained in Ref. [17] from the experimental data on the energy dependence of cross sections, averaged over the momentum distribution of the interacting particles obtained in the hadron gas model. The smallness of this averaged cross section led the authors of [17] to argue that strangeness phase space saturation would be too slow in a hadron gas. It is interesting that such a small value of the averaged cross section allows one to reproduce the observed enhancement of multistrange hyperons and antihyperons in central Pb-Pb collisions.

The main features of our results are the following: (1) The hyperon yields per participant increase faster than antihyperon ones. As a consequence, the ratio $R_Y = \overline{Y}/Y$ decreases between pPb and central Pb-Pb collisions; (2) The ratios R_Y increase with the number of strange quarks in the hyperon; (3) The increase of the Y and $\overline{Y}$ yields per participant is faster between pPb and the first centrality bin in Pb-Pb collisions and slows down between the first and last centrality bins of WA97. All these features are also present in the data.

Note added in proof. Preliminary data on the $\overline{p}$ yield at mid rapidities by the NA49 Collaboration have been presented at the Quark Matter 99 meeting (Torino, Italy, 1999). Together with published data on the Λ yield by the WA97 Collaboration in the same acceptance window, they indicate that the ration $\Lambda\overline{p}$ is significantly lower than one, in agreement with our predictions.

ACKNOWLEDGMENTS

It is a pleasure to thank N. Armesto, J. A. Casado, E. G. Ferreiro, A. B. Kaidalov, C. Pajares, and J. Tran Thanh Van for discussions. We also thank R. Lietava, P. Seyboth, and O. Villalobos Baillie for information on the data. A. C. acknowledges partial support from NATO Grant No. OUT-R.LG 971390. C.A.S. thanks Fundación Caixa Galicia from Spain for financial support.

[1] NA49 Collaboration, H. Appelshäuser *et al.*, nucl-ex/98110014.

[2] NA35 Collaboration, T. Albert *et al.* Eur. Phys. J. C **2**, 643 (1998); Z. Phys. C **64**, 195 (1994).

[3] DPM: A. Capella, U. Sukhatme, C.-I. Tan, and J. Tran Thanh Van, Phys. Lett. **81B**, 68 (1979); Phys. Rep. **236**, 225 (1994). A. Capella, U. Sukhatme, and J. Tran Thanh Van, Z. Phys. C **3**, 329 (1980); A. Capella and J. Tran Thanh Van, Phys. Lett. **93B**, 146 (1980); Z. Phys. C **10**, 249 (1981).

[4] QGSM: A. B. Kaidalov, Phys. Lett. **116B**, 459 (1982); *QCD at 200 TeV*, edited by L. Ciafarelli and Yu. Dokshitzer (Plenum, New York, 1992), p. 1; A. B. Kaidalov and K. A. Ter-Martirosyan, Phys. Lett. **117B**, 247 (1982).

[5] G. C. Rossi and G. Veneziano, Nucl. Phys. **B123**, 507 (1977).

[6] E. Gotsman and S. Nussinov, Phys. Rev. D **22**, 624 (1980).

[7] B. Z. Kopeliovich and B. G. Zakharov, Sov. J. Nucl. Phys. **48**, 136 (1988); Z. Phys. C **43**, 241 (1989); Phys. Lett. B **211**, 221 (1988).

[8] A. Capella and B. Kopeliovich, Phys. Lett. B **381**, 325 (1996).

[9] D. Kharzeev, Phys. Lett. B **378**, 238 (1996).

[10] HIJING: S. E. Vance, M. Gyulassy, and X. N. Wang, Phys. Lett. B **443**, 45 (1998).
[11] VENUS: K. Werner, Phys. Rep. **232**, 87 (1993); M. Hladik, Ph.D. thesis, Université de Nantes, 1998.
[12] A. Capella, E. G. Ferreiro, and C. A. Salgado, Orsay preprint LPT Orsay 99/06, hep-ph/9902232.
[13] NA49 Collaboration, H. Appelshäuser *et al.*, Phys. Lett. B **444**, 523 (1998).
[14] WA97 Collaboration, E. Andersen *et al.*,, Phys. Lett. B **433**, 209 (1998) CERN-EP/9929, Phys. Lett. B. (to be published).
[15] S. E. Vance and M. Gyulassy, nucl-th/9901009.
[16] A. Capella, Phys. Lett. B **387**, 400 (1996).
[17] B. Koch, B. Muller and J. Rafelski, Phys. Rep. **142**, 167 (1986).
[18] A. B. Kaidalov, Yad. Fiz. **45**, 1452 (1987) [Sov. J. Nucl. Phys. **45**, 902 (1987)]. A. B. Kaidalov and O. I. Piskunova, Z. Phys. C **30**, 141 (1986).
[19] B. Andersson, G. Gustafson, G. Ingelman, and T. Sjöstrand, Phys. Rep. **97**, 31 (1983); X. Artru, *ibid.* **97**, 147 (1983).
[20] A. Capella, A. Kaidalov, A. Kouider-Akil, C. Merino, and J. Tran Thanh Van, Z. Phys. C **70**, 507 (1996).
[21] H1 Collaboration, G. Adloff *et al.*, Proceedings of the 29th International Conference on High-Energy Physics, Vancouver, Canada, 1998.
[22] B. Kopeliovich and B. Povh, Phys. Lett. B **446**, 321 (1999).
[23] J. A. Casado, hep-ph/9810357.
[24] E. C. T. Alexopoulos *et al.*, Phys. Rev. D **46**, 2773 (1992).
[25] UA5 Collaboration, G. J. Alner *et al.*, Phys. Rep. **154**, 247 (1987).
[26] J. Ranft, A. Capella, and J. Tran Thanh Van, Phys. Lett. B **320**, 346 (1994); H. J. Möhring, J. Ranft, A. Capella, and J. Tran Thanh Van, Phys. Rev. D **47**, 4146 (1993).
[27] A. Capella, Phys. Lett. B **364**, 175 (1995).
[28] B. Koch, U. Heinz, and J. Pitsut, Phys. Lett. B **243**, 149 (1990).
[29] C. W. de Jager, H. de Vries, and C. de Vries, At. Data Nucl. Data Tables **14**, 479 (1974).
[30] N. Armesto and A. Capella, Phys. Lett. B **393**, 431 (1997); N. Armesto, A. Capella, and E. G. Fereiro, Phys. Rev. C **59**, 395 (1999).
[31] D. Kharzeev, C. Lourenço, M. Nardi, and H. Satz, Z. Phys. C **74**, 307 (1997).
[32] NA36 Collaboration, E. G. Judd *et al.*, Nucl. Phys. **A590**, 291 (1995).